

## ii-Preliminary Study in Diagnosis and Early Prediction of Preeclampsia by Using FTIR Spectroscopy Technique

Gehan A. Raouf<sup>1\*</sup>, Abdel-Rahman L. Al-Malki<sup>2</sup>, Nesma Mansouri<sup>3</sup>, Rogaia M. Mahmoudi<sup>4</sup>

<sup>1</sup>Medical Biophysics Lab., King Fahd Medical Research Centre; Biochemistry Dep., Faculty of Science, King Abdulaziz University, 21551 Jeddah –KSA B.O.Box:42805

<sup>2,4</sup>Biochemistry Dep., Faculty of Science, King Abdulaziz University, Jeddah –KSA

<sup>3</sup>Obstet. Gyneo. Dep., Faculty of Medicine, King Abdulaziz University, Jeddah–KSA

[gehan\\_raouf@hotmail.com](mailto:gehan_raouf@hotmail.com)

**Abstract:** Preeclampsia is a heterogeneous condition, potentially involving several separate pathophysiological pathways; currently no clinical screening test is useful for prediction of preeclampsia development. Fourier-transform infrared spectroscopy (FTIR) holds great promise for clinical chemistry measurements. FTIR spectra of plasma samples from pregnant women -14 patients and 31 normotensive were obtained. Second derivative spectra, Kramer Krong refractive index and ANOVA test were tacking in comparison studies. The parameters studied were proteins and lipids. Different absorbance ratios for specific bands were calculated and plotted versus the patient samples. The absorbance IR spectra of these two groups were slightly different, but from the curve fitting analysis, the protein secondary structure compositions were significant different. The decrease in  $\alpha$ -helix structure due to oxidative stress in patient group might be responsible of the dramatic increase in  $\beta$ -turns and unordered structure. Moreover, the peaks present in the IR second derivative, for patient group, at  $1744\text{cm}^{-1}$  (cholesterol and triglycerides ester C=O),  $1710\text{cm}^{-1}$  (carbonyl C-O stretch), and  $1621\text{cm}^{-1}$  (peptide C=O stretch) positively correlated with low density lipoprotein (LDL) oxidation. The results showed that among the normotensive control group three subjects later developed preeclampsia. Normotensive pregnant women who developed preeclampsia were considered as subjects at high risk. This study suggests, for the first time that FT-IR spectroscopy can be successfully used as an accurate and rapid test, for diagnosis and confirmed with 33% confidence level early prediction of preeclampsia, starting from 20 week of gestation.

[Gehan A. Raouf, Abdel-Rahman L. Al-Malki, Nesma Mansouri, Rogaia M. Mahmoudi. **ii-Preliminary Study in Diagnosis and Early Prediction of Preeclampsia by Using FTIR Spectroscopy Technique.** Journal of American Science 2011;7(4):827-836]. (ISSN: 1545-1003). <http://www.americanscience.org>.

**Keywords:** Fourier Transform Infrared Spectroscopy (FTIR); Oxidative Stress; Dyslipidemia; Preeclampsia; Plasma

**Abbreviations:** Fourier transform infrared spectroscopy (FTIR)

### Introduction

Preeclampsia, which affects 3% to 10% of pregnancies <sup>[1]</sup>, is a pregnancy-specific disorder characterized by hypertension, proteinuria and edema. The efforts to develop screening tests for potential use in clinical practice have yielded disappointing results <sup>[2]</sup>. Markers were generally chosen on the basis of specific pathophysiological abnormalities that have been reported in association with preeclampsia. Maternal concentrations of these biomarkers have been reported to be either increased or reduced early in gestation before the onset of preeclampsia. Given that preeclampsia is likely to be a heterogeneous condition, potentially involving several separate pathophysiological pathways, it is not surprising that simple clinical indicators are ineffective in identifying women who would benefit from pathway-specific treatment <sup>[3]</sup>. A variety of substances indicative of endothelial dysfunction are increased in the blood or urine of women with

preeclampsia <sup>[3, 4-5]</sup>. Many of these substances are elevated weeks before (as well as during) clinically evident preeclampsia <sup>[6,7]</sup>. It has been suggested that preeclampsia is a disease of antioxidant inadequacy appearing when the normal antioxidant balance is upset <sup>[8]</sup>.

During the last decade, Fourier transform infrared (FTIR) spectroscopy has proven and accepted to be a powerful tool for the study of biological samples. The primary reason for this is that common biomolecules such as proteins, nucleic acids, and lipids, have characteristic functional groups having unique molecular vibrational modes (vibrational fingerprints) corresponding to specific infrared light frequencies <sup>[9,10]</sup>. The composition and structure of molecular functional groups can be determined by analyzing the position, width, and intensity of infrared light absorption <sup>[12-16]</sup>.

In this cross sectiona study we have tested FTIR spectroscopy as a potential specific accurate

diagnostic tool for identifying normal pregnancy and preeclampsia, The second objective of this study was to define a new biophysical marker that is simple, valid and rapid, with potentially no limitation in clinical practice for early prediction of women – that are at high risk- who might later develop preeclampsia.

## 2. Materials and methods

This study was approved by the Bioethical and Research Committee at the Faculty of Medicine, King Abdulaziz University (KAU). An oral voluntary consent was obtained from all the participating subjects.

The main focus of this work was to conduct prospective or cross sectional studies aimed at evaluating the feasibility of using a clinical and biophysical test, performed during pregnancy, before the development of preeclampsia.

### Inclusion Criteria:

Cases eligible for inclusion in this study were normotensive pregnant women that have no evidence of proteinuria (control group) and patient group either with mild or severe preeclampsia. Preeclampsia was defined as hypertension (systolic blood pressure 140 mmHg and diastolic blood pressure 90 mmHg after 20 weeks' gestation) and proteinuria ( 300mg in a 24 hr urine collection or one dipstick measurement of 1+) according to the Committee off Terminology of American College of Obstetricians and Gynecologists (ACOG) definition<sup>[17]</sup>. Severe preeclampsia was diagnosed on the basis of diastolic blood pressure 110 mmHg or significant proteinuria (dipstick measurement of 2+) or the presence of severity evidences such as headache, visual disturbances, upper abdominal pain, oliguria, convulsion, elevated serum creatinine, thrombocytopenia, marked liver enzyme elevation, and pulmonary edema.

### Exclusion criteria:

Included fetal anomalies, chronic heart disease and inflammatory disorders.

### 2.1. Selection of women:

- **Age:** The age of 45 women participating in this study was from 16 to 49 years (mean= 32 years, SD= 7.6).

- **Week of gestation:** All the subjects were in second and third trimester. The gestational age was between 20 to 42 weeks. Data taken from the medical record of subjects are given in Table 1.

- **Study groups:** 31 normotensive pregnant women were taken as control group, and 14 patients diagnosed with preeclampsia were taken as the patients group. All subjects received obstetrical care at KAU hospital.

## 2.2. Blood Collection and plasma separation

Three ml of non-fasting vinous blood were drawn into in vacuoners test tubes containing ethylene diamine tetra-acetic acid (EDTA), an anti-clotting agent. The blood was immediately centrifuged at 4000 rpm for 10 min to separate plasma. The plasma was then removed and stored at -80 C. All the samples were first lyophilized prior to FTIR measurements.

## 2.3. Infrared Measurement

The lyophilized samples were dispersed in potassium bromide (KBr) by gently mixing with a pestle in an agate mortar to obtain a homogenous mixture as described in<sup>[14]</sup> but with 1% concentration. The mixture was then pressed in a die at 5 metric tons force for 3 s, creating a 1.1 cm diameter transparent disc with imbedded samples. For each sample, the absorbance of three different FTIR spectra were recorded at room temperature(26 C  $\pm$  1 C) in the mid infrared range (4000-400 cm<sup>-1</sup>) using a Shimadzu FTIR-8400s spectrophotometer with continous nitrogen purge. Those three spectra were then coadded. Typically, 20 scans were singal-averaged for a single spectrum and at spectral resolution of 4 cm<sup>-1</sup>. To minimize the difficulties arising from unavoidable shifts, baseline correction was applied by using IRsolution software. Each spectrum was normalized as normalization produces a spectrum in which maximum value of absorbance becomes 2 and minimum value 0 by using the same software. The parameters studied were proteins and lipids. After baseline correction, the best fit for decomposing the amide I bands in the spectral region of interest was obtained by Gaussian components using OMNIC software.

## 3. Results

### i) IR spectral features and assignments

The infrared spectra were obtained for 45 lyophilized plasma samples from pregnant women, including 31 samples from women clinically and laboratory assessed as healthy normotensive and 14 samples from patients already diagnosed as preeclampsia. Each spectrum was normalized and base line corrected.

This work is a continuous of our previous study on serum samples from the same subjects.<sup>[18]</sup> According to our previous findings based on the IR spectral signatures of serum and the calculated amide A/ Amide B ratio, the control spectra were successfully divided into two groups: control-1 (samples from 15-32) and control-2 (samples from 33-45; subjects are at high risk to develop preeclampsia).<sup>[18]</sup>

For clarity the sum, of equal numbers, of coadded spectra from control-1 samples, the sum of control-2 spectra and the sum of patient spectra are overlaid and shown in (Fig.1).

The main absorption bands in this figure belonging to lipids, proteins, carbohydrates and nucleic acids were defined in detail together with their assignments in Table 1.

Careful examination of the FTIR spectrum obtained from each sample revealed differences in the intensities of the absorption bands in relation to each other among the groups under investigation. It is obvious from Fig. 1 that control-1 & 2 spectra are almost indistinguishable, while the intensity of the entire spectrum of the patient group is markedly decreased compared to control-1 & 2 groups.

The intensity and/or more accurately the area of the absorption bands is directly related to the concentration of the molecules.<sup>[19, 20]</sup>

However, wide overlapping of bands in the raw spectrum causes difficulty in band segregation and their assignment. Hence using raw spectrum in the interpretation of data may not be totally conclusive, since the raw data obtained are often noisy.<sup>[21]</sup> Thus, in the present study, resolving this issue has been done by treating the raw spectrum with Kubelka Munk algorithm and later peak resolved for further interpretation. This method is used here for illustrative purpose only.

An advantage of this method is that the data is de-noised to a great extent.

Comparison of the IR spectra for control-1, control-2 and patient groups causes visualization in the band structure perturbation more distinctly.

Fig. 2 shows the curve-fitted amide I, amide II and esterified bands contour of all the tested groups. The data presented in Table 3 summarize the calculated positions and fractional areas of the amide I component bands from all groups under investigation. The amide I absorption is mainly associated with C=O stretching vibrations. The position of this absorption is sensitive to protein conformation.<sup>[22]</sup>

Table 3 showed a little decrease in  $\alpha$ -helix content (band around 1652cm<sup>-1</sup>) of amide I band for control-2 in respect to control-1 while there is no such band for patient group. On the other hand there is high content of  $\beta$ -turns and unordered protein secondary structure in patient group curve fitted spectra while there is no such structure in both control-1 and control-2 spectra.

## ii) Second Derivative Analysis

For further analysis, the second derivative spectra of plasma samples were obtained (Fig. 3) The most absorption peaks observed in both esterified

lipid (1750-1700 cm<sup>-1</sup>) and the amide I (1700-1600 cm<sup>-1</sup>) band and their assignment respectively are given in table 4. It is apparent from the Fig. 3(a) and the table that there is significant change in the bands positions and intensities which in turn will affect the plasma lipid profile and the secondary structure of plasma proteins as well.

The C=O stretching band (1739cm<sup>-1</sup>) is strongly associated with lipids implying that any shift in the frequency of this band can directly correlated with an alteration in the state of intramolecular hydrogen bonding of the interfacial region of the phospholipids structure with water molecules and/or some functional groups of other molecules.<sup>[23]</sup> In the current study, it has been observed that the spectrum of control-1 has an ill resolved bands and shoulders appeared as broad band in the range of 1738 – 1748 cm<sup>-1</sup>. In the control-2 spectrum this band apparently splits into one strong peak at 1741cm<sup>-1</sup> as well as a strong shoulder at 1748 cm<sup>-1</sup> while in patient spectrum only a strong band centered at 1744 cm<sup>-1</sup> is present. Moreover, the small band at 1710 cm<sup>-1</sup> becomes more intense and sharper in patient spectrum relative to the control-1. Meanwhile, it turned to a very weak shoulder together with the appearance of a new weak band at 1723 cm<sup>-1</sup> in the control-2 spectrum.

Examination of the second derivative spectra in the amide I region (1700-1600 cm<sup>-1</sup>) revealed that the over all plasma protein secondary structure consist mainly of  $\alpha$ -helix and anti parallel  $\beta$ -pleated sheets in control-1 as evident by the strong band centered at 1652 cm<sup>-1</sup> and 1690 cm<sup>-1</sup> respectively. Meanwhile, the main protein secondary structure in control-2 is antiparallel  $\beta$ -pleated sheets and random coil which was evident by the strong band centered at 1690 cm<sup>-1</sup> and 1645 cm<sup>-1</sup> respectively. On the other hand, the protein secondary structure for patient group consist mainly of  $\beta$ -sheets,  $\beta$ -turn and random coil indicated by the strong bands centered at 1687 - 1677 cm<sup>-1</sup>, 1664 and 1641 cm<sup>-1</sup> respectively.

## iii) Refractive Index Measurements:

Additional investigation to the second derivative spectra were performed by using IR solution software in calculating the refractive index (n) by using Kramers Kronig analysis. The (n) values for cholesterol band at 1470 cm<sup>-1</sup> is represented graphically in Fig. 4.

It is observed from the figure that the (n) values of most patient group are always higher >1.32 than control-1 & 2 groups. Moreover, the control-2 group has the lowest (n) values among the tested groups. These results were confirmed by results obtained from ANOVA test.

Comparison between these results and the information given in Table 1 was made and revealed the following:

1. The highest (n) value was obtained from patient numbers (1, 4, 6, 8, 10, 11, 12, and 14). They all had high BMI except patient numbers (4, 12), they were the youngest among this group.
2. For control-2 group, which showed the lowest (n) value among the tested groups, the sample

number (34) was exception. This subject developed later preeclampsia.

3. Samples number 35 and 39 also developed preeclampsia, they are 40 and 38 years old and their blood group for both are A<sup>+</sup>, although, they are at different gestational age.

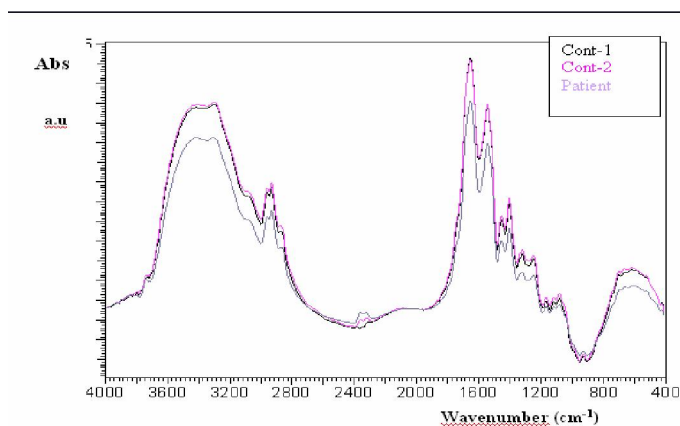


**Fig. 1.** FTIR spectra of plasma samples taken from control-1, control-2 and patient groups.

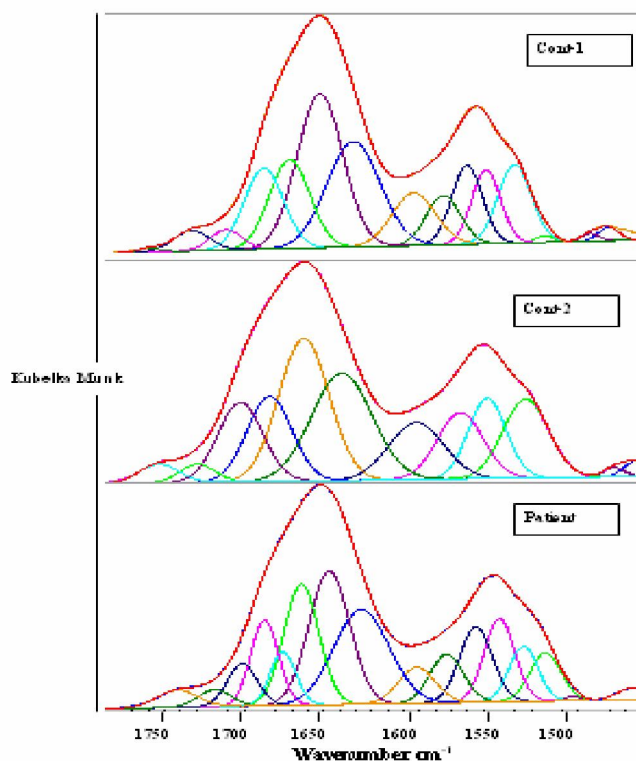


**Fig. 2.** Spectral curve-fitting of the 1800-1500 cm<sup>-1</sup> spectral interval of FTIR spectra of plasma samples from control-1, control-2 and patient groups.

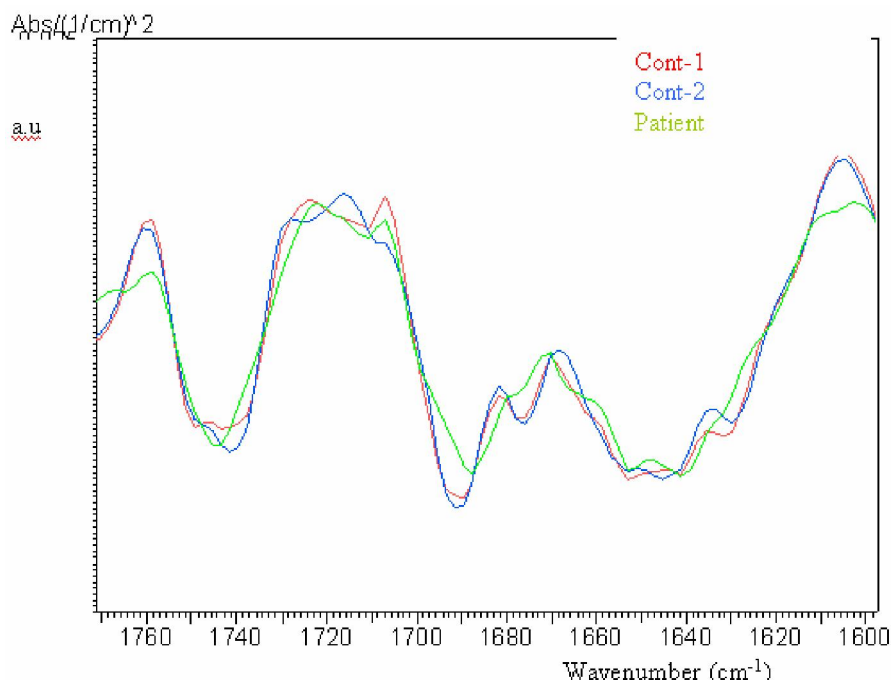


**Fig. 3.** IR second derivative spectra of plasma samples from control-1, control-2 and patient groups in range (1800-1400  $\text{cm}^{-1}$ ). The figure shows the shifts in the band positions and the changes in band intensities for esterified C=O(1750 -1700  $\text{cm}^{-1}$ ) and amide I bands (1700-1600  $\text{cm}^{-1}$ ) among control-1, control-2 and patient groups.

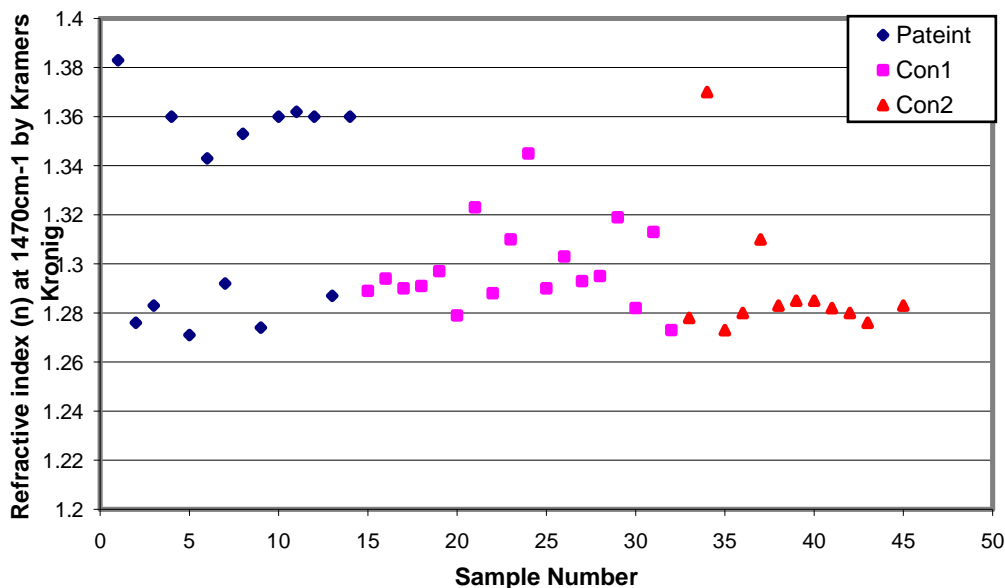


**Fig. 4:** Variation in the refractive index (n) among control-1, control-2 and patient groups in serum samples. The values are the average of three different measurements for each sample the SD ranging from 0.01- 0.008.

**Table 1: General information for subjects given from medical records in KAU hospital.**

Sample No	Gestation Age	Age	Blood Group	BMI	History	
Patients	1	42	30	O+	31.3	Mild PET, BP=147/89, protein= 0.12, SVD, fibrinogen, ALP, Neutrophils <b>medication</b> =aldomate 500 mg, adulate 20 mg.
	2	40	26	B+	30.0	Mild PET, BP=155/90,SVD, protein= 1.6, fibrinogen, ALP, Neutrophils, history preeclampsia, BP <b>medication</b> = adalate 20 mg.
	3	38	38	A+	35.0	Mild PET, BP= 139/84, GDM, hypertension, +ve protein urea, CS (trans lie verse baby).
	4	37	22	O+	24.3	Protein=0.162, BP=140/85, BP, fibrinogen, ALP, Neutrophils, PIH, <b>medication</b> =aldomate 250 mg.
	5	37	43	O+	43.2	BP, FDM, CS (brain aneurysm), LDL, cholesterol, protein= 0.15, ALP, Neutrophils, history preeclampsia, <b>medication</b> =omeprazole, glucophage 75 mg, omperazol, Insulin.
	6	37	43	O+	35.9	Mild PET, BP= 146/90, SVD, fibrinogen, ALP, LDH, history preeclampsia.
	7	37	26	A+	33.9	Mild PET, protein=0.399, BP= 147/85, protein=trace, fibrinogen, ALP, Neutrophils, history preeclampsia <b>medication</b> =omperazol 10 mg, aldamate 250 mg.
	8	36	31	A+	41.2	Mild PET, BP=144/80, 151/76, protein= 0.2, CS, TSH, fibrinogen, LDH, Eosinophils, history preeclampsia <b>medication</b> = thyroxin (hypothyroidism).
	9	35	37	B+	32.9	Mild PET, BP=150/90, protein=0.2, CS, previous PET, fibrinogen, ALP, AST, Neutrophils, <b>medication</b> =adalat 20 mg.
	10	34	27	A+	39.8	previous PET,CS, BP, GDM, <b>medication</b> = aldomat 250 mg.
	11	34	24	B+	36.0	BP= 149/90, 168/105, CS, fibrinogen, ALP, LDH, Neutrophils, <b>medication</b> = heparin, aldomt 500 mg.
	12	34	16	O+	23.9	Mild PET, BP= 146/84, protein= +2, SVD, wince, fibrinogen, ALP, LDH, AST, APTT, <b>medications</b> = adalat, ampecillin1 g.
	13	32	26	O+	-	SVD, Neutrophils, fibrinogen, <b>medications</b> = thyroxin.
	14	31	40	A+	36.0	Mild PET, BP= 148/65, protein= 0.28, fibrinogen, ALP, Neutrophils, <b>medications</b> = aldomat 250 mg.
Controls	15	37	37	B+	30.7	BP=115/67, SVD.
	16	37	46	B+	-	BP= 132/76, SVD, fibrinogen, ALP <b>medication</b> = ampecillin1 g.
	17	35	25	O+	-	BP= 104/48, CS.
	18	34	24	B+	-	BP= 95/52.
	19	33	29	A+	-	BP= 132/58.
	20	32	38	O+	38.1	BP= 97/63, CS.
	21	32	35	A+	29.8	BP= 117/55.
	22	30	20	A+	28.8	BP= 101/50.
	23	25	28	B+	34.8	BP= 92/56, SVD <b>medication</b> = thyroxin 25 mg (Hypothyroidism).
	24	25	36	O <sup>-</sup>	47.2	BP= 155/77, BP= 132/85, SVD.
	25	25	35	B+	-	BP= 107/57, CS.
	26	25	27	O+	42.8	BP= 102/53, SVD.
	27	24	27	O+	-	BP= 97/63, CS, Neutrophils.
	28	22	29	O+	28.2	BP= 117/55, twins, CS.
	29	22	22	A+	-	BP= 101/50.
	30	20	38	O+	-	BP= 92/56, SVD.
	31	20	36	O+	-	BP= 118/59, SVD.
	32	20	28	B+	-	BP= 100/63, CS.
	33	38	43	O+	27.2	BP= 121/76, SVD, anemia during pregnancy, Neutrophils, ALP <b>medications</b> = Erythromycin 500 mg.
	34	22	21	O+	16.7	BP= 110/56, SVD. TSH, glucose, AST, Neutrophils, Basophils.
	35	20	40	A+	33.4	BP= 121/82, CS, Neutrophils, Eosinophils, Fibrinogen, APTT.



36	20	27	O+	24.7	BP= 90/55, Neutrophils.
37	35	32	B+	-	BP= 113/60, CS.
38	35	33	O+	-	BP= 135/87, GDM, SVD, BP, history with disease.
39	35	38	A+	27.4	BP= 109/59, kidney disease, total protein, posterior vaginal repair.
40	33	38	O+	28.0	BP= 122/78, anemia during pregnancy, SVD.
41	25	28	B+	37.1	BP= 118/74, CS, Eosinophils.
42	25	42	O+	-	BP= 113/75, SVD, hyperglycemia.
43	24	49	O+	-	BP= 139/67, diabetes, history preeclampsia, BP, CS, medications=aldomat.
44	24	31	O+	27.3	BP= 113/66, ALP.
45	21	27	A+	-	BP= 96/63, kidney disease, Neutrophils, Eosinophils, Fibrinogen, APTT.

**Table 2: Major plasma assignments from plasma FT-IR spectra absorption bands.**

Bands (cm <sup>-1</sup> )	Major assignments
3020-3000	(CH): unsaturated fatty acids, cholesterol esters
2990-2950	as(CH <sub>3</sub> ): cholesterol esters, triglycerides
2950-2880	as(CH <sub>2</sub> ): long chain fatty acids, phospholipids
2880-2860	s(CH <sub>3</sub> ): cholesterol esters, triglycerides, glycerol
2870-2830	s(CH <sub>2</sub> ): long chain fatty acids, phospholipids
2996-2819	as(CH <sub>3</sub> ), s(CH <sub>3</sub> ), as(CH <sub>2</sub> ), s(CH <sub>2</sub> ): fatty acids, phospholipids, triglycerides
1739-1732	(C=O): lipid, cholesterol, triglycerides
1720-1600	(C=O): (amide I) -sheet: proteins, turns, coils
1630-1560	(NH <sub>2</sub> ):amino acids
1600-1480	(N-H):(amide II) -helix: proteins
1480-1430	as(CH <sub>3</sub> ), as(CH <sub>2</sub> ), s(CH <sub>3</sub> ), s(CH <sub>2</sub> ): fatty acids, phospholipids, triglycerides
1430-1360	(COO): amino acids
1300-900	(C-O): saccharides, glucose, lactate, glycerol

: stretching vibrations, : bending (scissoring) vibrations, s: symmetric, as: asymmetric. Spectral assignment taken from references [9-12, 15,16].

**Table 3: positions and fractional areas of the amide I component bands for plasma samples taken from control-1, control-2 and patient groups.**

Peak centre (cm <sup>-1</sup> )	Structure	Cont-1	Cont-2	patient
<b>1626.411</b>	<b>-turns</b>	-	-	<b>69.89</b>
1630.022	Parallel -sheets	79.14	83.76	
1646.592	unordered structure	-	-	72.75
<b>1653.095</b>	<b>-helix</b>	<b>99.41</b>	<b>92.78</b>	
<b>1664.177</b>	<b>-turns</b>	-	-	<b>56.54</b>
1674.014	Parallel -sheets	50.71	49.32	18.25
1687.300	-sheets	-	-	31.79
1691.718	Anti-parallel -sheets	44.67	46.22	

Spectral assignment was taken from references [22, 47].

**Table 4: Second derivative component bands of the esterified region 1750-1700cm<sup>-1</sup>.**

Control-1	Control-2	patient	Band assignment	Ref.(Masayuki et al., 2002)
w 1711	w sh 1717	-		vLDL & LDL
w sh 1726	-	w 1725	hydrogen-bonded C=O groups	
m 1738	m 1738	-	Ester C=O	LDL
m 1748	m 1748	s 1741	non-hydrogen bonded ester carbonyl C=O	vLDL

w=weak, sh=shoulder, m=medium, s=strong [42,43]

#### 4. Discussion

It has been suggested that preeclampsia is a disease of antioxidant inadequacy appearing when the normal antioxidant balance is upset.<sup>[8]</sup> Oxidative damage by free radicals or reactive oxygen species (ROS) can result in lipid peroxidation and protein modification [24] causing changes in membrane properties and cell dysfunction.<sup>[25]</sup> The highly reactive primary products of lipid peroxidation, lipid hydroperoxides, are formed when free radicals attack polyunsaturated fatty acids or cholesterol in membrane and lipoproteins. Lipid hydroperoxides function in normal physiology by regulating enzymes and redox-sensitive genes<sup>[26, 27]</sup>. However, uncontrolled lipid peroxidation like in case of preeclampsia can result in cellular dysfunction and damage.<sup>[1, 28, 29]</sup> Such damage, known as oxidative stress, is normally prevented by an extensive and multilayered antioxidant system consisting of both low and high molecular weight components.<sup>[24]</sup>

It was previously suggested that free radical damage can cause a reduction in protein synthesis.<sup>[30]</sup> Albumin may represent the major and predominant circulating antioxidant in plasma [31], which is known to be exposed to continuous oxidative stress<sup>[32]</sup>. Alterations in the structure of albumin may result in impairments of its biological properties<sup>[33]</sup>.

On the bases of the forgoing consideration, one can explain the significant decrease in the protein peaks intensities together with the observed band shifts in plasma samples for patient group compared to control-1 & 2. Thus, a dramatic change in proteins secondary structure takes place which in turn impair the antioxidant effect of serum albumin and blood circulating antioxidant. These changes occurred earlier and were more pronounced in the women whom preeclampsia later developed. Our results are also agreed with results obtained by (Fraile et al., 2003).<sup>[34]</sup> They observed that the Amide II/ Amide I ratio is higher for pure albumin as compared with Albumin-lipid systems. Their results revealed that lipids destabilize albumin native structure.

IR spectroscopy support at least modification of secondary structure in albumin upon addition of lipids [34]. The derivative gave the number and positions, as well as an estimation of the bandwidth and intensity of the bands making up the amide I region.

It should be mentioned here that although patients either with mild or severe preeclampsia are under medication but the IR second derivative spectra and protein secondary structure obtained from amide I components are also capable to differentiate all groups under investigations. The decrease in  $\alpha$ -helix structure of plasma protein might be responsible for the increase in  $\beta$ -turns structure in patient group.

During pregnancy, maternal lipids are elevated to supply the developing fetus with triglycerides and cholesterol<sup>[35]</sup> exaggerated lipid changes have been reported in women with preeclampsia. These differences have been documented both before and after clinical manifestations of preeclampsia.<sup>[35-38]</sup> Some investigators have suggested that dyslipidemia may contribute to the increased oxidative stress and endothelial dysfunction observed in preeclampsia.<sup>[36]</sup>

Plasma concentrations of very low density lipoprotein (VLDL) and LDL increase progressively with gestational age as reflected by increases in serum triglycerides and cholesterol.<sup>[39, 40]</sup> Gestational increases in estrogen are thought to promote hepatic production of VLDL triglyceride.<sup>[41]</sup> The patient group enrolled in this study were classified either with mild or severe preeclampsia (Table 1). Accordingly, the marked increase in the values of refractive index for the patient group at the band  $1475\text{ cm}^{-1}$  over the control 1 and 2 groups may be attributed to the significant higher triglycerides and higher total cholesterol to HDL ratio than controls. Since obesity, age, diabetes and kidney disease are all important risk factors for preeclampsia, we examined wither alteration in this parameters could account for the elevated the refractive index (n) values. We have demonstrated that there is significant increase in (n) values in some patient and control-2 groups those with high BMI and/or young age. The blood group O<sup>+</sup> and A<sup>+</sup> might play a role in increasing the risk factor<sup>[18]</sup>, but this point should be studied in further details and with large sample number. It should be mentioned here that the increase in (n) value  $> 1.32$  for cholesterol can be considered as strong evidence and biomarker in diagnosis and early prediction of disease. On the other hand, the decrease in (n) values are not necessary prove of healthy pregnancy and normal cholesterol, TG and glucose level in plasma.

The present study has shown that the region of ester C=O stretch ( $1750\text{-}1700\text{ cm}^{-1}$ ) can be used as a marker for characterizing triglycerides (TG) and cholesterols, which are the main components for VLDL and LDL, respectively. The C=O stretching bands for unsaturated (TG) and unsaturated cholesterol exhibit a band at about  $1746$  and  $1738\text{ cm}^{-1}$ , respectively.<sup>[42]</sup> The peaks at  $1745$  (cholesterol and triglycerides ester C=O),  $1710$  (carbonyl C-O stretch), and  $1621\text{ cm}^{-1}$  (peptide C=O stretch) positively correlated with LDL oxidation.<sup>[43]</sup> According to the above mentioned data, the appearance of a very strong band at  $1741\text{ cm}^{-1}$  and a medium band at  $1710\text{ cm}^{-1}$  in patient plasma samples together the shoulder at  $1622\text{ cm}^{-1}$  or  $1626\text{ cm}^{-1}$ , in plasma samples IR second derivative and amide I component obtained from curve fitting respectively,



can be attributed to the oxidation of LDL during preeclampsia. (Morris et al., 1998)<sup>[44]</sup> found no evidence that circulating lipid peroxidation products (8-iso-PGF<sub>2</sub>, lipid hydroperoxides, and malondialdehyde) are elevated in preeclampsia once appropriate precautions were taken, including addition of antioxidants, to prevent in vitro oxidation. This finding disagreed with our results which showed that even preeclamptic women under medication their IR second derivative spectra gave the observed proatherogenic changes in lipid profile. Proatherogenic lipid profiles have been demonstrated in women months before clinical signs of preeclampsia.<sup>[45]</sup> Triglyceride levels are elevated, high density lipoprotein (HDL) levels tend to be lower, and small dense low-density lipoprotein (LDL) particles are higher in preeclampsia compared with normal pregnancies [35-38] this shift in LDL particle size to smaller and denser subfractions is thought to be particularly important, as these are highly susceptible to oxidation and may play a critical role in the endothelial dysfunction seen in preeclampsia.<sup>[28, 35]</sup> All of these proatherogenic changes in the lipid profile are also found in cardiovascular disease and diabetic subjects and represent those at high risk for coronary artery disease.<sup>[46]</sup>

Data from larger number of subjects throughout the pregnancy are needed for better assess the relevance of these markers to the diagnosis and early prediction of preeclampsia.

## 5. Conclusion

In summary, we have demonstrated a marked increase in cholesterol, TG and glucose in plasma begging 4- 8 weeks before the onset of preeclampsia, and accompanied by decreases in the protein intensity bands. This study together with our previous study on serum gives promising biophysical marker. The change in protein secondary structure, the changes in lipid profile together with the elevated refractive index for the 1475cm<sup>-1</sup> band could help in diagnosis and early prediction of preeclampsia. Thus, samples number 34 (one out of 31 normotensive control subjects) developed preeclampsia later, she was at 22 week of gestation. In addition, this study demonstrated that FTIR spectroscopy can be used in clinical analysis as a rapid and sensitive tool for studying human biofluids and biomolecules.

## Acknowledgments

This research work was supported by King Abdulaziz City for Science and Technology grant number M.S.11-23.

## Corresponding Author:

Gehan Abdel-Raouf Mohamed Fouad Ahmed

Address: King Abdulaziz University, Faculty of Science, Biochemistry Department-Jeddah-Kingdom of Saudi Arabia (KSA) P.O Box: 42805 Postal code: 21551; Email: [jahmed@kau.edu.sa](mailto:jahmed@kau.edu.sa); [gehan\\_raouf@hotmail.com](mailto:gehan_raouf@hotmail.com)

## References

1. Carl A, Oxidative stress in the Pathogenesis of preeclampsia. 1999; 222-235
2. Francois A, Screening for pre-eclampsia: the quest for the holy grail? *The Lancet* 2005; 365(9468) : 1367-1369.
3. Villar J, Say L, Shennan A, Lindheimer M, Duley L, Conde-Agudelo A, Merialdi M, Methodological and technical issues related to the diagnosis, screening, prevention, and treatment of pre-eclampsia and eclampsia. *Int. J. Gynecol. Obstet.* 85 Suppl.1 2004; S28-S41.
4. Taylor R.N, Roberts JM, Endothelial cell dysfunction. In: Lindheimer MD., Roberts JM, Cunningham FG, EGs. *Chesley's Hypertensive Disorders in Pregnancy* (2<sup>nd</sup> ed.) Stamford, CT: Appleton & Lange, pp395-429, 1999.
5. Roberts J, Endothelial dysfunction in preeclampsia. *Sem Report Endocrinol.* 1998;16: 5-15.
6. Krauss T, Juhn W, Lakoma C, Augustin HG, Circulating endothelial cell adhesion molecules as diagnostic markers for the early identification of pregnant women at risk for development of preeclampsia. *Am. J. Obstet. Gynecol.* 1997; 177: 443-449.
7. Taylor RN, Crombleholme WR, Friedman SA, Jones LA., Casal DC, Roberts JM, High plasma cellular fibronectin levels correlate with biochemical and clinical features of preeclampsia but cannot be attributed to hypertension alone. *Am. J. Obstet. Gynecol.* 1991; 165: 895-901.
8. Stark J, Preeclampsia and cytokine induced oxidative stress. *Br. J. Obstet. Gynecol.* 1993; 100: 105-9.
9. Carmona P, Rodriguez-Casado A, Alvarez I, de Miguel E, Toledano A, FTIR microspectroscopic analysis of the effect of certain drugs on oxidative stress and brain structure. *Biopolymer* 2008;89:548-554.
10. Dumas P and Miller J, The use of synchrotron infrared microspectroscopy in biological and biomedical investigations. *Vib. Spec.* 2003;32:3-21.
11. Griffiths PR, and de Haseth JA, *Fourier transform infrared spectrometry.* John Wiley and Sons, New York, 45, 1986.
12. Jakson M and Mantsch HH, In Mantsch H.H., Chapman D. (eds.), *Infrared spectroscopy of biomolecules,* Wiley-Liss, Toronto, 311, 1996.
13. Baker MJ, Gazi E, Brown MD, Shanks JH, Gardner P, and Clarke NW, FTIR-based spectroscopic analysis in the identification of clinically aggressive prostate cancer. *British J. Cancer* 2008; 99: 1859-1866.
14. Paul GL, Robert DS, Cancer grading by Fourier transform infrared spectroscopy. 1998;4: 37-46.
15. Jackson M, Sowa MG, Mantsch HH, Infrared spectroscopy: a new frontier in medicine. *Biophys. Chem.* 1997; 68: 109-125.
16. Diem M, Boydston-White S, & Chiriboga L, Infrared spectroscopy of cells and tissues: shining light on a novel subject. *Appl. Spectrosc.* 1999; 53: 148A-161A.

17. Cuningham FG, Gant NF, Leveno KJ, Gilstrap III LC, Hauth JC, Wenstrom KD, Williams Obstetrics. 21 st Ed. McGraw-Hill 2001; 568-9.
18. Gehan A. Raouf, Abdel-Rahman L. Al-Malki, Nesma Mansouri, Rogaia M. Mahmoudi, ii-Preliminary Study in Diagnosis and Early Prediction of Preeclampsia by Using FTIR Spectroscopy Technique Life Sci. J. 2011 (accepted).
19. Severcan F., Gorgulu G., Gorgulu T.S., Guray T., Anal. Biochem. 2005; 339: 36
20. Toyran N., Zorlu F., Donmez G., Ode K.L., Severcan F. Eur. Biophys. J. 2004;33: 549.
21. Sasic S., Morimoto M., Otsuka Y., Two-dimensional correlation spectroscopy as a tool for analyzing vibrational images. *Vibr. Spec.* 2005;37: 217-24
22. Palaniappan PL. and Vijayasundaram V., The FT-IR study of the brain tissue of Labeo rohita due to arsenic intoxication. *Microchemical J.* 2009;91:118-124.
23. Takahshi H., French S. & Wong P., Alteration in hepatic lipids and proteins by chronic ethanol intake: A high pressure Fourier transform infrared spectroscopic study on alcoholic liver disease in the rat. *Alcoholism-Clinical and Experimental Res.* 1991;15: 219-223.
24. Sinclair A, Barnett A, Lunec J, Free radicals and antioxidant systems in health and disease. *Br. J. Hosp. Med.* 1990; 43: 334-344.
25. Corinne M, John R, Ewen W, Rhoda W, James J, James Mc, Erythrocyte glutathione balance and membrane stability during preeclampsia. *Free Radical Biol. Med.* (1998); 24(6): 1049-1055.
26. Smith WL, Marnett LJ, DeWitt DL, Prostaglandin and thromboxane biosynthesis. *Pharmacol Ther.* 1991; 49: 153-179.
27. Sen CK, Packer L, Antioxidant and redox regulation of gene transcription. *FASEB J* 1996;10: 709-720.
28. Hubel CA, Roberts JM, Taylor RN, Musci TJ, Rogers GM, McLaughlin MK, Lipid peroxidation in pregnancy: New perspectives on preeclampsia. *Am. J. Obstet. Gynecol.* 1989; 161:1025-1034.
29. Walsh SW, Maternal-placental interactions of oxidative stress and antioxidants in preeclampsia. *Sem Reprod Endocrinol.* 1998; 16: 93-104.
30. Makrides S. C., Protein-synthesis and degradation during aging and senescence. *Biological Reviews* 1983;58: 343-422.
31. Halliwell B, How to characterize a biological antioxidant, *Free Radic. Res. Commun.* 1990; 9: 1-32.
32. Soriani M, Pietraforte D, Minetti M, Antioxidant potential of anaerobic human plasma: role of serum albumin and thiols as scavengers of carbon radicals, *Arch. Biochem. Biophys.* 1994;312: 180-188.
33. Terawaki H, Yoshimura K, Hasegawa T, Matsuyama Y, Negawa T, Yamada K, Matsushima M et al, Oxidative stress is enhanced in correlation with renal dysfunction: examination with the redox state of albumin, *Kidney Int.* 2004;66: 1988-1993.
34. Fraile M, Blanco-Melgar, Martinez R, Lopse G, Gallego J, Carmona P, Structure and interactions of albumin-Lipid Systems as studied by infrared spectroscopy. *J. M. Strac.* 2003; 651-653: 231-236.
35. Sattar N, Bedomir A, Berry C, Shepherd J, Greer IA, Packard C, Lipoprotein subfraction concentrations in preeclampsia: pathogenic parallels to atherosclerosis. *Obstet. Gynecol.* 1997; 89: 403-8.
36. Lorentzen B, Endresen M, Clausen T, Henriksen T, Fasting serum free fatty acids and triglycerides are increased before 20 weeks of gestation in women who later develop preeclampsia. *Hypertens Pregnancy* 1994; 13: 103-9.
37. Chappell L, Seed P, Briley A, et al., A longitudinal study of biochemical variables in women at risk of preeclampsia. *Am. J. Obstet. Gynecol.* 2002; 187:127-36.
38. Gratacos E, Casals E, Sanllehy C, Cararach V, Alonso P, Fortuny A, Variation in lipid levels during pregnancy in women with different types of hypertension. *Acta Obstet. Gynecol. Scand.* 1996; 75: 896-901.
39. Knopp RH, Bonet B, Lasuncion MA, Montelongo A, Herrera E. Lipoprotein metabolism in pregnancy. In: Herrera E, Knopp R, Eds. *Perinatal Biochemistry.* Boca Raton, FL: CRC Press, Inc., pp20-51, 1992.
40. Potter JM, Nestel PJ. The hyperlipidemia of pregnancy in normal and complicated pregnancies. *Am J Obstet Gynecol.* 1979;133:165-170.
41. Alvarez JJ, Montelongo A, Iglesias A, Lasuncion MA, Herrera E. Longitudinal study on lipoprotein profile, high-density lipoprotein subclass, and postheparin lipases during gestation in women. *J Lipid Res.* 1996;37 :299-308.
42. Masayuki N, Mitsuyo O, Hiroyuki K, Infrared study of human serum very low-density and low-density lipoproteins. Implication of esterified lipid C=O stretching bands for characterizing lipoproteins. *Chem. Phys. Lipids* 2002; 117(1-2): 1-6.
43. Henry SL, Andrew P, John N, Manford D, Grady W, Quantitative determination of low density lipoprotein oxidation by FTIR and chemometric analysis. *Lipids* 2004; 39(7): 687.
44. Morris JM, Gopaul NK, Endresen MJ, Knight M, Linton EA, Dhir S, Anggard EE, Redman CW, Circulating markers of oxidative stress are raised in normal pregnancy and preeclampsia. *Br. J. Obstet. Gynaecol.* 1998; 105:1195-1199.
45. Arthur M, Richard L, Kevin L, Sina H, and Boggess K, Maternal serum dyslipidemia occurs early in pregnancy in women with mild but not severe preeclampsia. *Am. J. Obstet. Gynecol.* 2009 ;201:293.
46. Carmena R, Duriez P, Fruchart J, Atherogenic lipoprotein particles in atherosclerosis. *Circulation* 109 (suppl 1) 1112-1117. View Record in Scopus Cited By in Scopus (87).
47. Cyril P. and Gerard D., Chemical mapping of tumor progression by FT-IR imaging: towards molecular histopathology. *TENDS in Biotech.* 2006;24(10): 455-462.

4/8/2011